Hypernitrosylated ryanodine receptor/calcium release channels are leaky in dystrophic muscle

Andrew M. Bellinger, Steven Reiken, Christian Carlson, Marco Mongillo,

Xiaoping Liu, Lisa Rothman, Stefan Matecki, Alain Lacampagne,

and Andrew R. Marks

Supplementary Figure 1

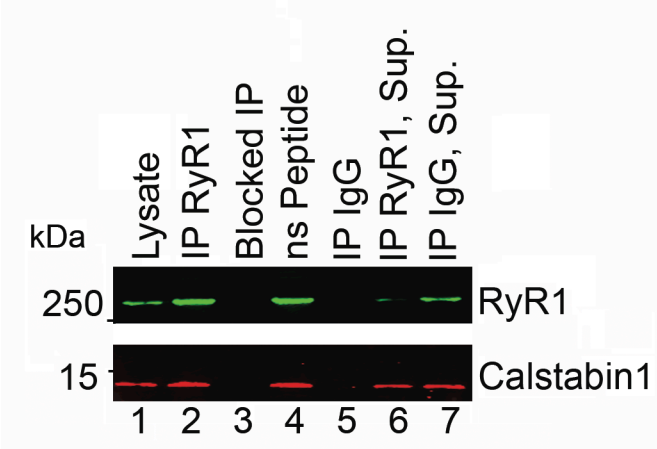

Supplemental Figure: **Immunoprecipitation (IP) of RyR1 with isoform-specific antibody**

Lane 1, Immunoblot of RyR1 and calstabin1 using EDL lysate (25 μg); lane 2, RyR1 and calstabin1 co-immunoprecipitated from 250 μg EDL muscle lysate in a total of 500 μl of RIPA buffer using an RyR1 isoform specific antibody and Protein A beads; lane 3, blocking the RyR1 IP with the antigenic peptide that was used to generate the RyR1-specific antibody; lane 4, no blocking of the RyR1 IP using a non-specific peptide (100:1 peptide:antibody molar ratio for both peptides), demonstrating antibody specificity; lane 5, IP with IgG used as a negative control; lane 6, RyR1 IP supernatant indicating nearly complete IP; lane 7, 10% of the IgG IP supernatant (equivalent to 25 μg of lysate) showing that the amounts of RyR1 and calstabin1 in lanes 1 and 7 are equivalent. Following IP, samples were centrifuged for 1 min at 1,000 X g. The supernatants were collected and the beads were washed 3X with RIPA buffer. EDL lysate (25 μg),

the IPs, and supernatants were size-fractionated using a 6% PAGE for RyR1 and 15% PAGE for calstabin 1. There is calstabin1 in the RyR1 IP supernatant and the IgG supernatant because in addition to being bound to RyR1 calstabin1 is also present in the cytosol of muscle.

Supplemental Methods

Animals and S107 treatment. S107 (S107-HCl FW 245.77) was synthesized as previously described [1,2]. The structure and purity of S107 were confirmed by NMR, MS, and Elemental Analysis [1]. The specificity of S107 was assessed by extensive testing of activities against a panel of >250 channels, receptors, phosphatases and kinases, and the drug was shown to require calstabin1 because its beneficial effects on exercise capacity were not observed in skeletal muscle specific calstabin1 deficient mice [1]. Age-matched *mdx* and WT mice littermates were sacrificed as indicated for analysis of the RyR1 macromolecular complex. Four parallel, blinded trials of S107 treatment of *mdx* mice were performed. All assays were not performed on all S107 treated and vehicle controls, though each measurement was balanced pair wise with respect to treatment within each trial. Mice were housed in a pathogen-free facility and standard food and water were provided *ad libitum* throughout the experiment.

Measurement of EDL resistance to contraction-induced mechanical stress. Supramaximal stimuli with a monophasic pulse duration of 3 ms were delivered using a computer-controlled electrical stimulator (model S44; Grass Instruments) connected in series to a power amplifier (model 6824A; Hewlett Packard). Muscle force was displayed on a storage oscilloscope (Tektronix S.A.), and the data were simultaneously acquired to computer (The Dynamic Muscle Control/Data Acquisition (DMC) and the Dynamic Muscle Control Data Analysis (DMA) programs, Aurora Scientific Inc.) via an analog-to-digital converter at a sampling rate of 1000 Hz. The EDL was adjusted to the optimal length (L_0, the length at which maximal twitch force is achieved), and supramaximal stimulation at 100 Hz for 600 ms was performed. The muscle was held at L_0 during the initial 400 ms (isometric component) and then lengthened to 115% of L_0 for 200 ms (eccentric component). Peak muscle length was maintained for 100 ms after the cessation of electrical stimulation, followed by a return to L_0 for 100 ms (see **Fig. 4a**). After a 60-s recovery period, a 100-Hz isometric stimulation was performed at L_0 to determine isometric force production after one eccentric contraction. Developed isometric force following the eccentric contraction was normalized to the peak muscle force developed prior to the eccentric contraction and expressed as per cent decrease in force [3]. Endurance protocol (30 Hz 300 ms trains every second for 300 s) (see **Fig. 4i**). We normalized force values to the force developed during the first train of the protocol.

Voluntary exercise measurements. Wheel revolutions were continuously

recorded using a cycle counter BC600 Sigma sport for 72 hr. For each animal, the experimental procedure started between 12:30 and 1:00 pm to reduce the variability associated with diurnal rhythms. In addition, mice were placed in the cage 5 days prior to the experiments to acclimate to the environment and the wheel.

Calcium sparks measurements. Following in situ contractile measurements, mice were euthanized and EDL muscles were dissected and stored in a HEPES-buffered physiological medium (in mM: 119 NaCl, 5 KCl, 1.25 $CaCl_2$, 1 $MgSO_4$, 10 glucose, 1.1 mannitol, 10 HEPES, pH 7.4). Muscles were then rapidly placed in a dissecting chamber and the solution exchanged with a relaxing solution (in mM: 140 K-glutamate, 10 HEPES, 10 $MgCl_2$, 0.1 EGTA, pH 7.0). Bundles of 5 to 10 EDL fibers were manually dissected, mounted as described previously [4] and permeabilized in a relaxing solution containing 0.01% saponin for 30 s. After washing with saponin free solution, the solution was changed to an internal medium for imaging: (in mM) 140 K-glutamate, 5 Na_2ATP, 10 glucose, 10 HEPES, 4.4 $MgCl_2$, 1.1 EGTA, 0.3 $CaCl_2$, Fluo-3 0.05 pentapotassium salt (Invitrogen), pH 7.0, for sparks acquisition as previously reported [5,6]. Potential sparks were empirically identified using an autodetection algorithm [7]. The number of sparks examined were n = 615, 2586 and 883 in WT, vehicle treated mdx and mdx mice treated with S107 respectively). The mean F0 value for the image was calculated by summing and averaging the temporal F at each spatial location while ignoring potential spark areas. This F0 value was then used to create a smoothing routine, potential spark locations were visualized and analyzed for spatiotemporal properties as described previously [8]. Image analysis was performed using IDL (v5.5, Research System, Inc.). Statistical comparisons were performed using an ANOVA test with a significance level set at $P<0.05$ (Sigmastat v3.5).

RyR1 biochemistry. Five mg EDL muscle samples from WT and *mdx* age-matched littermates were isotonically lysed. RyR1 was immunoprecipitated from 250 μg of homogenate using an anti-RyR antibody (4 μg RyR1-1327) in 0.5 ml of a modified RIPA buffer (50 mM Tris-HCl pH 7.4, 0.9% NaCl, 5.0 mM NaF, 1.0 mM Na_3VO_4, 1% Triton-X100, and protease inhibitors) for 1 hr at 4°C. The immune complexes were incubated with protein A Sepharose beads (Amersham Pharmacia) at 4°C for 1 hr and the beads were washed three times with buffer. Proteins were separated on SDS-PAGE gels (4-20% gradient) and transferred onto nitrocellulose membranes for 2 hr at 200 mA (SemiDry transfer blot, Bio-Rad). To prevent non-specific antibody binding, the membranes were incubated with blocking solution (LICOR Biosciences) and washed with Tris-buffered saline with 0.1% Tween-20. After three washes, membranes were incubated with infrared-labeled secondary antibodies (1:10,000, LICOR Biosystems). Band intensities were quantified using the Odyssey Infrared Imaging System (LICOR Biosciences). Levels of RyR1 PKA phosphorylation, RyR1 S-nitrosylation, and bound calstabin1 were normalized to the total RyR1 immunoprecipitated

(arbitrary units). Control samples were analyzed on each gel to for normalization. Total RyR1 levels were not different between genotype or treatment group.

RyR1 S-nitrosylation and NOS isoforms. SR vesicles (25 μg) from rabbit skeletal muscle were incubated with either NOR-3 (50 μM, 500 μM, Calbiochem) or NOC-12 (100 μM, 1000 μM, Calbiochem) in a 50 mM MOPS-NaOH buffer (pH 7.4) containing 50 μM $CaCl_2$ and 300 mM NaCl for 30 min at RT. Following incubation, the vesicles were washed three times with the MOPS buffer with centrifugation at 100,000 x g for 10 min between each wash. Samples were analyzed for total RyR1, S-nitrosylated RyR1, and calstabin1 by 4-20% PAGE as described above. In order to investigate the potential role of NOS enzymes, the levels of iNOS and eNOS were compared between *mdx* and WT muscle homogenates. Muscle homogenates were separated by 4-20% PAGE and immunoblots were developed with antibodies to iNOS (1:2000), eNOS, or nNOS (1:1000, VWR). In addition, iNOS and eNOS were immunoprecipitated from 250 μg of homogenate using antibody to iNOS (5 μL) or antibody to eNOS (5 μL) as described above. Immunoprecipitates were washed and size-fractionated by 4-20% PAGE followed by immunobloting with antibodies to RyR1 and NOS enzymes as indicated. Antibody to RyR1 was pre-incubated with its peptide antigen (1:100 molar ratio) for 1 hour at RT for the peptide blocked co-immunoprecipitation.

Immunohistochemistry. Immunohistochemistry was performed to determine whether RyR1 and iNOS co-localize in murine skeletal muscle from *mdx* mice. EDL was removed, washed in physiological solution, incubated for 10 min in relaxing buffer containing (in mM): 100 KCl, 5 EGTA, 5 $MgCl_2$, 3 2,3-butanedione monoxime, 0.25 dithiothreitol, 10 histidine, pH 7.8, and then snap-frozen in isopentane cooled in liquid nitrogen. Muscles were embedded according to standard procedures in Jung Tissue Freezing Medium (Leica Microsystems) at –20°C and sectioned using a microtome to produce 6-10 μm-thick sections, which were placed on electrostatically charged microscope slides. Sections were then fixed in paraformaldehyde (4%), quenched in NH_4Cl (50 mM), and incubated with 2% BSA-PBS for 30 min at RT before incubation with the RyR1-specific antibody (1:500) and the antibody to iNOS (1:100; R&D Systems) followed by treatment with anti-mouse and anti-rabbit IgG conjugated with Alexa-Fluor-488 and Alexa Fluor-568 (Invitrogen). After mounting the cover slips in Slow Fade-Gold DAPI (Invitrogen), images were acquired using a fluorescence microscope (Apotome, Carl Zeiss Microimaging).

Analysis of mdx muscle fibers treated with S107. Analysis of % of muscle fibers with central nucleation in diaphragm was performed on n = 300 WT, 286 *mdx* vehicle, 309 *mdx* S107 fibers. Distribution of fiber cross sectional areas in diaphragm from vehicle-treated *mdx* and S107-treated *mdx* S107 treatment was measured as thousands of μm^2 using n=300 WT, 286 *mdx* vehicle treated, 309 *mdx* S107 treated fibers from 3 animals for each condition.

Creatine Kinase Assay

Blood was collected at the time of sacrifice by intracardiac puncture in heparinized mice, centrifuged at 4,000 rpm for 5 min, and the serum was immediately frozen at -80 °C. Serum samples (duplicates, 5 µl each) were added to 200 µl of CK reagent (Pointe Scientific, Inc.) and the absorbance at 340 nM was recorded over 4 min.

1. Bellinger, A., Reiken, SR, Dura, M, Murphy, P, Deng, S-X, Neiman, D, Lehnart, S, Samaru, M, LaCampagne, A, and Marks, AR Remodeling of ryanodine receptor complex causes "leaky" channels: a molecular mechanism for decreased exercise capacity *PNAS* **105**, 2198-2202 (2008).
2. Wehrens, X.H.*, et al.* Protection from cardiac arrhythmia through ryanodine receptor-stabilizing protein calstabin2. *Science* **304**, 292-296 (2004).
3. Petrof, B., Shrager, J., Stedman, H., Kelly, A. & Sweeney, H. Dystrophin protects the sarcolemma from stresses developed during muscle contraction. *Proc Natl Acad Sci U S A* **90**, 3710-3714 (1993).
4. Lacampagne, A., Klein, M.G. & Schneider, M.F. Modulation of the frequency of spontaneous sarcoplasmic reticulum Ca^{2+} release events (Ca^{2+} sparks) by myoplasmic [Mg^{2+}] in frog skeletal muscle. *J Gen Physiol* **111**, 207-224 (1998).
5. Reiken, S.*, et al.* PKA phosphorylation activates the calcium release channel (ryanodine receptor) in skeletal muscle: defective regulation in heart failure. *J Cell Biol* **160**, 919-928 (2003).
6. Ward, C.W.*, et al.* Defects in ryanodine receptor calcium release in skeletal muscle from post-myocardial infarct rats. *Faseb J* **17**, 1517-1519 (2003).
7. Cheng, H.*, et al.* Amplitude distribution of calcium sparks in confocal images: theory and studies with an automatic detection method. *Biophys J* **76**, 606-617 (1999).
8. Lacampagne, A., Ward, C.W., Klein, M.G. & Schneider, M.F. Time course of individual Ca^{2+} sparks in frog skeletal muscle recorded at high time resolution. *J Gen Physiol* **113**, 187-198 (1999).